Prion-like Conformational Editing of SMN2 Proteins Rescues Spinal Muscular Atrophy

I-Fan Wang (ifanwang.gbs@gmail.com)
Garage Brain Science

Chen-Hung Ting
1. Marine Research Station, Institute of Cellular and Organismic Biology, Academia Sinica

Li-Kai Tsai
Department of Neurology, National Taiwan University Hospital and National Taiwan University College of Medicine

Hsiang-Yu Chang
Garage Brain Science

Hsing-Jung Lai
National Taiwan University Hospital and National Taiwan University College of Medicine

Chien-Lin Chen
Department of Neurology, National Taiwan University Hospital and National Taiwan University College of Medicine

Biological Sciences - Article

Keywords: survival motor neuron (SMN) proteins, spinal muscular atrophy (SMA), prion-like LC domain, liquid-liquid phase separation (LLPS), gems and Baicalein.

Posted Date: June 11th, 2021

DOI: https://doi.org/10.21203/rs.3.rs-606188/v1

Abstract

Spinal muscular atrophy (SMA) causes the loss of motor neurons and progressive muscle weakness. In 95% of patients with SMA, both alleles of the survival motor neuron 1 (*SMN1*) gene are deleted or the gene contains missense mutations. A nearly identical copy of *SMN1*, *SMN2*, is normally expressed but is unable to compensate for the loss of *SMN1* due to the deletion of exon 7. Here, we demonstrated that conformational editing of the SMN2 protein triggers effective phase separation of SMN2 proteins and rescues SMA. We found that SMN1 contains a prion-like LC domain at exons 6-7, which drives liquid-liquid phase separation (LLPS) and further discovered an LLPS activator of gems, baicalein. Using baicalein, we reinvented SMN2 proteins into a competent prion-like conformation to restore the prion-like functions of SMN1 and effectively rescue SMA mice. Our study suggests that the impaired prion-like activity of SMN1 is the root cause of SMA and provides a drug candidate for SMA and phase separation-deficient diseases.

Introduction

Spinal muscular atrophy (SMA) is an autosomal recessive neuromuscular disorder that affects approximately 1 in 10,000 babies born worldwide each year[1, 2]. Deficiencies in the SMN protein result in a gradual loss of motor neurons in the anterior horn of the spinal cord and subsequent system-wide atrophy of skeletal muscles[3]. The gene responsible for SMA, survival motor neuron 1 (*SMN1*), has been identified[4]. A nearly identical copy of the gene, *SMN2*, is normally expressed in all patients with SMA. Although a small amount of full-length protein is produced that is identical to *SMN1*, the exon-splicing silencer bearing a C-to-T transition in exon 7 of *SMN2* in all individuals skips exon 7[5, 6]. The protein product SMNΔ7 appears to be unstable and rapidly degrades[9]. Increasing the copy number of *SMN2* modulates the severity of SMA but does not fully compensate for the loss of *SMN1*[7, 8]. Although *SMN1* was identified as the mutant gene responsible for SMA 20 years ago, the molecular mechanisms by which exon 7 deletion alters cellular functions and SMA-associated mutations trigger the disease have not been elucidated.

Several misfolded disease-causing proteins harbor an intrinsic prion-like domain, which recently has been suggested to play numerous roles in normal cellular processes, such as membrane-less granule organization, alternative splicing and heterochromatin formation, underlying liquid-liquid phase separation (LLPS) via temporal homo- and hetero-cross-β polymerization (prion-like interactions)[10,11,12,13,14]. Similar to known prion-like low complexity (LC) proteins, SMN concentrates in subnuclear bodies called gems and is incorporated into cytosolic stress granules (SGs) through interaction with a prion-like protein, TIA1[15, 16]. Interestingly, Lorson et al. identified a modular self-oligomerization region in exon 6 of SMN, and the disease severity was inversely proportional to the intracellular concentration of oligomerization-competent SMN proteins and the formation of gems[17]. Given that the membrane-less granule organization and self-oligomerization are the signature of prion-like LC proteins, we thus hypothesized that the SMN is a prion-like protein and the deficiency in prion-like

functions of SMN leads to SMA. Indeed, we identified that SMN contains a prion-like LC domain at exons 6-7, which drives LLPS, and discovered an LLPS activator of gems, baicalein. We found that baicalein reinvented the C-terminus of the SMNΔ7 protein transcript encoded by *SMN2* into a competent prion-like conformation, restored the prion-like function of SMN and effectively rescued SMA mice.

An Activator of SMN Associated with Phase Separation Rescues SMA

Dysfunctional targeting of SMN to gems and coiled bodies (CBs) has been suggested to be a feature of SMA in patients[18]. In searching for a phase separation-associated activator to rescue SMA, we found that baicalein restores the assembly of gems in SMA patient-derived human dermal fibroblasts (HDFs) by screening a chemical library (Fig. 1a). The statistical analysis of the effect of baicalein on gem body formation is shown in Fig. 1b. To determine whether the *in vitro* findings could be recapitulated *in vivo*, we treated a late-onset mouse model of SMA (type III) with daily intraperitoneal injections of baicalein (13.6 mg/kg/d) or DMSO (control). After 4 weeks of treatment, histological analysis of the lumbar spinal sections of SMA mice confirmed an increase in ChAT-positive motor neuron numbers (Fig. 1c, P=0.0435) and recovery of nuclear gems (Fig. 1c, bottom, labeled by arrowheads, P=0.0063).

We found that the SMN protein levels were increased in various tissues of baicalein-treated SMA mice compared with those in control SMA mice (Fig. 1d, e), but the *SMN* mRNA levels were not (Extended Data Fig. 1), affirming that baicalein may increase the protein stability of SMND7. Beginning at 7 months of age, we next treated the type III SMA mice with baicalein for four months, which improved mouse survival (P=0.048) (Fig. 1f). A reduction in the evoked compound muscle action potential (CMAP) amplitude upon sciatic nerve stimulation was observed in control SMA mice (Fig. 1g, left, P=0.0201), but this phenomenon was prevented in baicalein -treated SMA mice (Fig. 1g, right, P=0.3326). Baicalein-treated SMA mice showed better motor performance than control mice in both the fixed-speed and accelerating rotarod tests, measuring the latency to fall (Fig. 1h and i). Fluorogold retrograde tracing of spinal motor neurons revealed a higher motor neuron density within the anterior horn (Fig. 1j, top, P=0.0114) and more large a-motor neurons (Fig. 1j, bottom, P=0.0037) in baicalein-treated mice than in control SMA mice. Significantly, baicalein treatment improved the axonal innervation of neuromuscular junctions (NMJs) in the hamstring muscles of SMA mice (Fig. 1k, P=0.04).

We also treated an early-onset mouse model of SMA (type I) with daily intraperitoneal injections of baicalein (13.6 mg/kg/d) or DMSO (control) beginning at birth. After baicalein treatment, the functional performances of the SMA mice, including their righting times, tube scores, and tilting scores, were improved on the 6th postnatal day (P<0.05), and the results were similar to those of their heterozygous littermates treated with or without baicalein. On the 8th postnatal day, the functional performances of the baicalein-treated SMA mice were better than those of the untreated SMA mice in the tube test (P=0.009) but not in the turnover test (P=0.065) or negative geotaxis test (P=0.58) (Extended Data Fig. 2). However, baicalein-treated type I SMA mice showed lifespans (8.8±0.4 vs. 7.9±0.2 days; P=0.13) and body weight gains that were similar to those in control SMA mice. We assumed that the limited therapeutic impact of baicalein on type I SMA mice may have been due to the shortened treatment duration.

Liquid-liquid Phase Separation of SMN

Biotinylated isoxazole (b-isox), a recently identified specific chemical probe, specifically recognizes the cross-β prion-like polymer and sequentially precipitates with proteins harboring prion-like, low-complexity or phase-separated domains, such as TDP-43, Fus and tau[11]. To determine whether SMN is a prion-like LC protein, we initially incubated 100 mM b-isox with lysates of mes23.5 and 293T cells at 4°C to chemically precipitate whole prion-like proteins and then analyzed the efficiency of SMN binding by Western blot to assess the prion-like and phase transition potentials of SMN (Fig. 2a). Western blot analysis revealed the precipitation of SMN by b-isox (Fig. 2a). Subcellular fractionation analysis further revealed that the major conformation of SMN recognized by the b-isox was localized in the cytosol (Fig. 2b). SET and PFN1 were used as fractionation controls (Fig. 2b). The sumoylated SMN proteins known to associate with the formation of gems, were the predominant SMN conformations detected in nuclear soluble and insoluble urea fractions[19]. H3K4me3 proteins were used as controls for insoluble loading (Fig. 2c). The insoluble sumoylated proteins of SMN disappeared following b-isox treatment (Fig. 2c). Consistently, we treated healthy HDFs with b-isox and found that the number of gems was significantly reduced in a dose-dependent manner, confirming that prion-like LC interactions of SMN constitute gems (Extended Data Fig. 3). We deduced that sumoylation is a cellular regulatory mechanism that triggers the separation phase of nuclear SMN though cross-β polymerization.

To determine prion-like domain of SMN, we examined the LLPS capabilities of full-length SMN (SMN-FL) and a panel of exon-deleted SMN constructs. The map of the SMN variants and results are shown in Fig. 2d. Only fragments containing the region encoding exons 6-7 formed visible granules (Fig. 2e, arrowhead). The dynamics of mCherry-$SMN_{exon6-7}$ granules in living cells were further analyzed by time-lapse microscopy, and the trajectory of mCherry-$SMN_{exon6-7}$ granules is shown in Fig. 2f. Most of the mCherry-$SMN_{exons6-7}$ granules traveled within a limited location (Fig. 2f), and two independent granules of mCherry-$SMN_{exon6-7}$ occasionally underwent fission and fusion (Fig. 2g, arrowheads). The average granular speed of mCherry-$SMN_{exon6-7}$ was ~0.8 μm/s. As the prion-like domain of SMN is localized at exons 6-7, we inferred that the deletion of exon 7 leads to insufficient prion-like activity of SMN protein.

Prion-like Conformational Editing of SMNΔ7 Proteins by Baicalein

As the SMA patient-derived HDFs and SMA type III mice shown in Fig. 1 express only the SMN2 proteins, we speculated that baicalein restores gems in SMA patient-derived HDFs and SMA type III mice by editing the conformation of the C-terminus of SMNΔ7. Using the b-isox precipitation assay to detect the *in vivo* cross-β conformation of SMN, we found that the cross-β conformers of SMN in HDFs and SMA patient-derived HDFs were different (Fig. 3a). Importantly, the cross-β conformers of SMNΔ7 in SMA patient-derived HDFs were recapitulated as cross-β conformers of SMN-FL upon baicalein treatment (Fig. 3a). This result supported that baicalein can edit the conformation of SMNΔ7 into a prion-like conformer of SMN1 and explain the pharmacological mechanism of baicalein in restoration of the formation of gems in Figure 1a and 1c. In order to assess whether the prion-like activity of SMNΔ7 *per se* increases upon baicalein, we performed coimmunoprecipitation to analyze the prion-like interactions of SMNΔ7 and

PFN1. PFN1 is a aggregation-prone protein co-precipitates with b-isox, and known to effectively interact with SMN but not SMNΔ7 (Fig. 2b) [20, 21, 22]. The results showed that in the presence of baicalein, the interactions between PFN1 and SMNΔ7 were significantly increased (Fig. 3b). As the prion-like conformation is critical for the protein stability of TDP-43, we next examined whether baicalein attenuated the degradation of the SMNΔ7 protein, and it indeed significantly reduced SMNΔ7 degradation (Fig. 3c, arrow). In a previous study, neurons transfected with SMNΔ7 extended significantly shorter neurites than those transfected with SMN-FL[23, 24]. Baicalein increased the length of axons from NSC34 cells expressing SMNΔ7 by approximately 2-fold (Fig. 3d); the statistical analysis is shown in Fig. 3e. These results together with those in Fig. 1 suggest that baicalein endows SMNΔ7 with prion-like bioactivity. We notice that two patient-derived missense SMN1 mutants, Y272C and G279V, mutated in exon 6 increased the binding affinity of the b-isox and the insolubility. Change in these two biochemical properties reflected that their cellular conformation was altered (Extended Data Fig. 4). These results suggested that amino acids 272 and 279 and exon 7 are critical for the adoption of a competent prion-like conformation of SMN, and the impaired prion-like activity of SMN1 is the root cause of SMA.

To validate the role of prion-like activity in SMA, we increased the amount of functional prion-like domains by overexpressing the TDP-43 prion-like domain (TDP-43-PLD) in NSC34 motor neuron cells expressing the SMNΔ7 protein to confirm that the level of the functional prion-like conformer affects axon degeneration. TDP-43-PLD is expected to adopt a common, structurally similar cross b-sheet to compensate for the prion-like function of SMN. Our experiment showed an increase in axon length in cells expressing both SMNΔ7 and GFP-TDP-43 PLD compared to the GFP- and GFP-NPLD-expressing controls (Fig. 3f, arrowheads). The statistical analysis is shown in Fig. 3g. Conversely, SMN overexpression in motor neurons has also been shown to slow the onset of amyotrophic lateral sclerosis (ALS) and pathological symptoms in a model of mutant TDP-43[25, 26, 27]. Thus, the level of the prion-like conformer is critical for motor neuron survival, and other functionally unrelated prion-like proteins can compensate for the function of the defective protein.

Based on the unique role of prion-like conformations in motor neurons, we propose a therapeutic model of SMA, “the prion-like conformation-based therapies”, in which SMA disease-causing mutants and SMNΔ7 are converted into prion-like folded proteins (Fig. 3h). Baicalein endowed SMN mutants and SMNΔ7 with prion-like activity, subsequently triggering LLPS of SMNΔ7 to form gems and increasing prion-like interactions, i.e. SMNΔ7-PFN1, reducing protein degradation of SMN, and improving motor neuron survival and motor functions in SMA patients.

Discussion

The strong correlation between the self-association of the SMN protein[3,8] and disease severity suggests that SMN self-oligomerization is a prerequisite for essentially all SMN functions[17]. Here, we discovered that the self-oligomerization of SMN is driven by an intrinsic prion-like conformation, defining SMA as a conformational disease. SMNΔ7 has lost its ability to adopt a prion-like conformation, accounting for the

inability of *SMN2* to compensate for the loss of *SMN1*[17]. Unlike the wide spectrum of conformational disease-causing proteins related to neurodegeneration, such as mutated TDP-43 and tau, the structure of the SMNΔ7 protein renders it subject to rapid degradation rather than the formation of pathological inclusions[28]. We thus propose a group of conformational diseases that has not yet been identified, in which prion-like defective proteins are rapidly degraded.

By increasing the levels of the SMN-FL protein in spinal motor neurons, three approved therapies Zolgensma (Novartis), Spinraza (Biogen) and risdiplam (Roche) have been effective in clinical testing so far, but the prices of the SMA drugs are up to $2 million- world's most expensive drug [29, 30, 31]. Our studies provide a simple method for compensating the prion-like functions of the SMN1 protein by modulating the folding of the SMN2 C-terminus to ensure that the protein of SMN2 performs the prion-like cellular functions (or LLPS) of SMN-FL. We termed these reassembled prion-like conformers of SMN2 as prion-like iso-conformers (Fig. 3h). Orally administrated drug baicalein is a therapeutic expected to significantly mitigate the severity of motor dysfunction and deaths in SMA, and may lead to lower SMA drug prices over the long term.

Declarations

Acknowledgments

We thank the staff at the Image Core at Academia Sinica and the First Core Labs at National Taiwan University for their assistance with the confocal microscopy and technical support. The SMN constructs were kindly gifted by Dr. Li-Hung at IMB, Academia Sinica. We dedicate this work to Dr. Hung-Li and commemorate and thank him for inspiring our academic careers. This research was funded by Garage Brain Science (ND-01-002) and was supported by the Ministry of Science and Technology in Taiwan to Dr. L.-K. Tsai (108-2314-B-002-082-MY3).

Author Contributions: H.-Y. Chang conducted the characterization of the prion-like properties of SMN. C.-H. Ting analyzed axonal outgrowth. C.-L. Chen, H.-J. Lai, and L.-K. Tsai performed the SMA animal experiments and pharmacological analysis. I.-F. Wang initiated and coordinated the project and performed the research. H.-Y. Chang, C.-H. Ting, L.-K. Tsai and I.-F Wang wrote the manuscript, which was approved by all co-authors.

Conflict of Interest Statement

H.-Y. Chang, C.-H. Ting and I.-F Wang are financially compensated as employees of Garage Brain Science.

References

1. Brzustowicz, L. M. et al. Genetic mapping of chronic childhood-onset spinal muscular atrophy to chromosome 5q11.2-13.3. *Nature*. **344**, 540-541 (1990).

2. Melki, J. et al. Gene for chronic proximal spinal muscular atrophies maps to chromosome 5q. *Nature*. **344**, 767-768 (1990).
3. Bussaglia, E. et al. A frame-shift deletion in the survival motor neuron gene in Spanish spinal muscular atrophy patients. *Nat Genet*. **11**, 335-337 (1995).
4. Lefebvre, S. et al. Identification and characterization of a spinal muscular atrophy-determining gene. *Cell*. **80**, 155-165 (1995).
5. Monani, U. R. et al. A single nucleotide difference that alters splicing patterns distinguishes the SMA gene SMN1 from the copy gene SMN2. *Hum. Mol. Genet*. **8**, 1177–1183 (1999).
6. Le, T. T. et al. SMNDelta7, the major product of the centromeric survival motor neuron (SMN2) gene, extends survival in mice with spinal muscular atrophy and associates with full-length SMN. *Hum. Mol. Genet.* **14**, 845-857 (2005).
7. Burnett, B. G. et al. Regulation of SMN protein stability. *Mol. Cell. Biol*. **29**, 1107–1115 (2009).
8. Monani, U. R. et al. The human centromeric survival motor neuron gene (SMN2) rescues embryonic lethality in Smn(−/−) mice and results in a mouse with spinal muscular atrophy. *Hum. Mol. Genet*. **9**, 333–339 (2000).
9. Vitali, T. et al. Detection of the survival motor neuron (SMN) genes by FISH: further evidence for a role for SMN2 in the modulation of disease severity in SMA patients *Hum. Mol. Genet.* **8**, 2525–2532 (1999).
10. Wang, I. F. et al. The self-interaction of native TDP-43 C terminus inhibits its degradation and contributes to early proteinopathies. *Nat Commun.* **3**, 766 (2012).
11. Kato, M. et al. Cell-free formation of RNA granules: low complexity sequence domains form dynamic fibers within hydrogels. *Cell.* **149**, 753-767 (2012).
12. Kwon, I. et al. Phosphorylation-regulated binding of RNA polymerase II to fibrous polymers of low-complexity domains. *Cell*. **155**, 1049-1060 (2013).
13. Xiang, S. et al. The LC Domain of hnRNPA2 Adopts Similar Conformations in Hydrogel Polymers, Liquid-like Droplets, and Nuclei. *Cell*. **163**, 829-839 (2015).
14. Strom, A. R. et al. Phase separation drives heterochromatin domain formation. *Nature.* **547**, 241-245 (2017).
15. Morse, R. et al. Targeting of SMN to Cajal bodies is mediated by self-association. *Hum Mol Genet*. **16**, 2349-2358 (2007).
16. Hua, Y., & Zhou, J. Survival motor neuron protein facilitates assembly of stress granules. *FEBS Lett*. **572**, 69-74 (2004).
17. Lorson, C. L. et al. SMN oligomerization defect correlates with spinal muscular atrophy severity. *Nat Genet.* **19**, 63-66 (1998).
18. Hebert, M. D., Szymczyk, P. W., Shpargel, K. B. & Matera, A. G. Coilin forms the bridge between Cajal bodies and SMN, the spinal muscular atrophy protein. *Genes Dev*. **15**, 2720-2729 (2001).

19. Tapia, O. et al. The SMN Tudor SIM-like domain is key to SmD1 and coilin interactions and to Cajal body biogenesis. *J Cell Sci.* **127**, 939-946 (2014).
20. Giesemann, T. et al. A role for polyproline motifs in the spinal muscular atrophy protein SMN. Profilins bind to and colocalize with smn in nuclear gems. *J Biol Chem.* **274**, 37908-37914 (1999).
21. Sharma, A. et al. A role for complexes of survival of motor neurons (SMN) protein with gemins and profilin in neurite-like cytoplasmic extensions of cultured nerve cells. *Exp Cell Res.* **309**, 185-197 (2005).
22. Wu, C. H. et al. Mutations in the profilin 1 gene cause familial amyotrophic lateral sclerosis *Nature*. **488**, 499-503 (2012).
23. Dodds, E., Dunckley, M. G., Roberts, R. G., Muntoni, F. & Shaw, C. E. Overexpressed human survival motor neurone isoforms, SMNDeltaexon7 and SMN+exon7, both form intranuclear gems but differ in cytoplasmic distribution. *FEBS Lett.* **495**, 31-38 (2001).
24. Zhang, H. L. et al. Active transport of the survival motor neuron protein and the role of exon-7 in cytoplasmic localization. *J Neurosci.* **23**, 6627-6637 (2003).
25. Perera, N. D. et al. Enhancing survival motor neuron expression extends lifespan and attenuates neurodegeneration in mutant TDP-43 mice. *Hum Mol Genet.* **25**, 4080-4093 (2016).
26. Turner, B. J. et al. Survival motor neuron deficiency enhances progression in an amyotrophic lateral sclerosis mouse model. *Neurobiol Dis.* **34**, 511-517 (2009).
27. Yamazaki, T. et al. FUS-SMN protein interactions link the motor neuron diseases ALS and SMA. *Cell Rep.* **2**, 799-806 (2012).
28. Neumann, M. et al. Ubiquitinated TDP-43 in frontotemporal lobar degeneration and amyotrophic lateral sclerosis. *Science*. **314**, 130-133 (2008).
29. Hua, Y. et al. Enhancement of SMN2 exon 7 inclusion by antisense oligonucleotides targeting the exon. *PLoS Biol.* **5**, e73 (2007).
30. Hahnen, E. et al. Missense mutations in exon 6 of the survival motor neuron gene in patients with spinal muscular atrophy (SMA). *Hum Mol Genet.* **6**, 821-825 (1997).

Figures

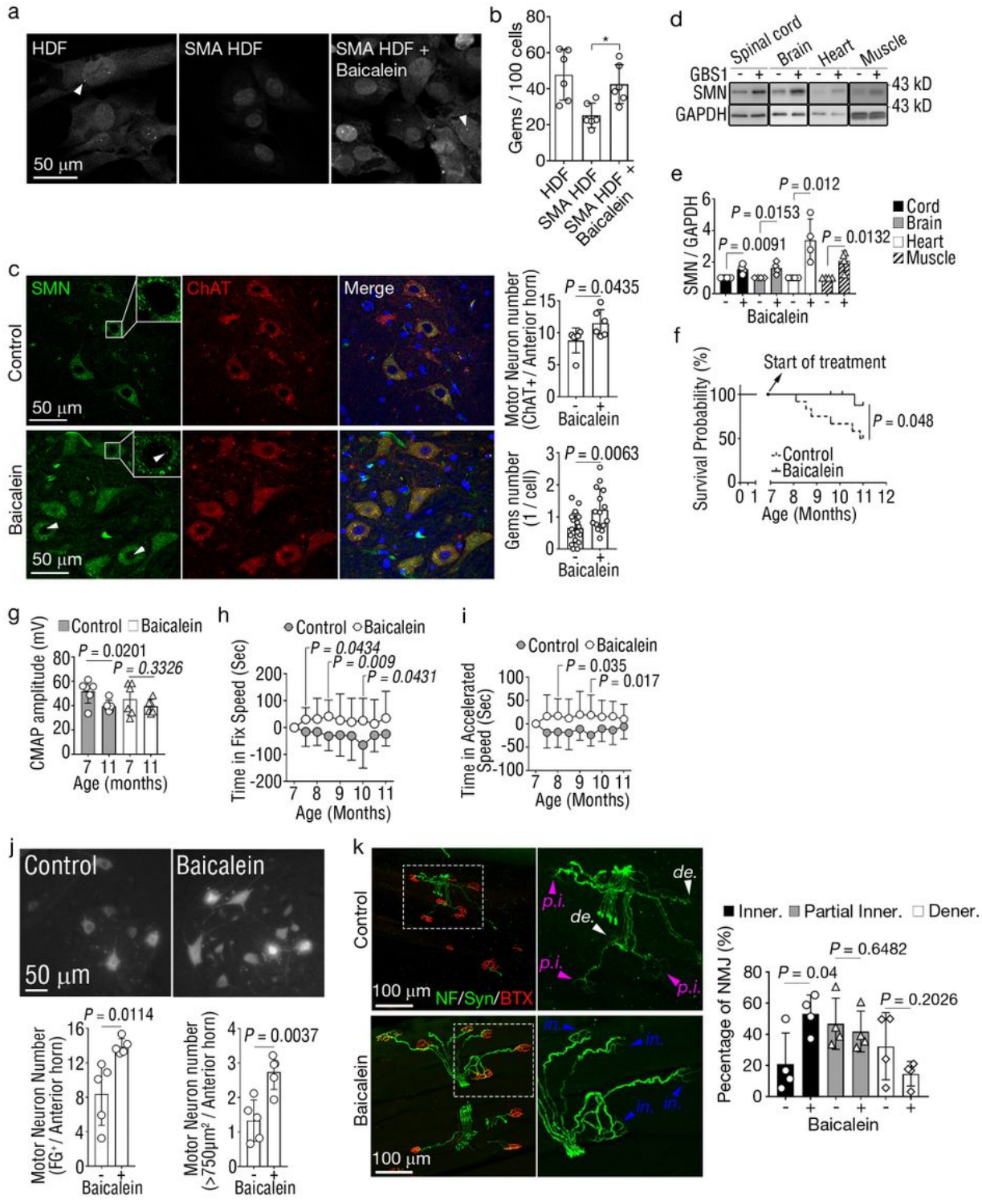

Figure 1

Baicalein Rescues Gems and Motor Neuron Functions in SMA Patient-derived HDFs and SMA Mice a, Immunofluorescence images of gems in wild type (WT) and SMA patient-derived human dermal fibroblasts (HDFs) with or without baicalein treatment. The arrowhead indicates gem bodies. Scale bars: 50 μm. b, Statistical analysis of gem numbers in WT and SMA patient-derived HDFs with or without baicalein treatment. All the data are presented as the mean with standard deviation (SD) (n= 6). *P < 0.05

by t-test. c, Histological staining of lumbar spinal motor neurons in SMA mice with or without baicalein treatment using anti-ChAT (red), anti-SMN (green), and DAPI (blue). The magnified region is shown in boxes to the right of the SMN panel, where the arrowheads show nuclear gems. Bar: 50 mm. Right, quantifications of ChAT-positive motor neuron and nuclear gem counts (per cell) in the anterior horn of SMA mice; n = 6 in each group. d, Western blot analysis of the Smn expression in various tissues of SMA mice treated with or without baicalein daily for 2 weeks. e, Quantitation of the Smn expression relative to GAPDH as shown in (e); n = 4 in each group. f, Survival analysis of SMA mice treated with (n = 10) or without (n = 12) baicalein daily for four months beginning at 7 months of age. g, Comparison of compound motor action potential (CMAP) amplitudes between results at 7 (baseline) and 11 months of age in SMA mice with or without baicalein treatment; n=6 in each group. h-i, Latency to fall from the fixed-speed (h) and accelerating (i) rotarod tests in baicalein-treated (n = 10) and control (n = 12) SMA mice. The values presented were normalized to the baseline data. j, Retrograde tracing of lumbar spinal motor neurons using intramuscular injection of fluorogold (FG) in SMA mice treated with or without baicalein for 4 months. Bottom, quantifications of the FG-positive motor neuron and large a-motor neuron (area > 750 mm2) counts. Bar, 50 μm; n = 5 in each group. k, Staining with neurofilament-H/synaptophysin (green) and a-bungarotoxin (BTX) (red) reveals neuromuscular junctions (NMJs) in SMA mice. Bar: 100 mm. The magnified region is shown on the right, demonstrating nerve innervation (in.), partial innervation (p.i.), or denervation (de.) of NMJs. Right, quantification of NMJ patterns; n = 4 in each group. e,g,j,k, Unpaired two-tailed Student’s t-test. f, Gehan-Breslow-Wilcoxon test. h,i, multiple t-test. The data are shown as the means ± SD, and P values < 0.05 were considered significant.

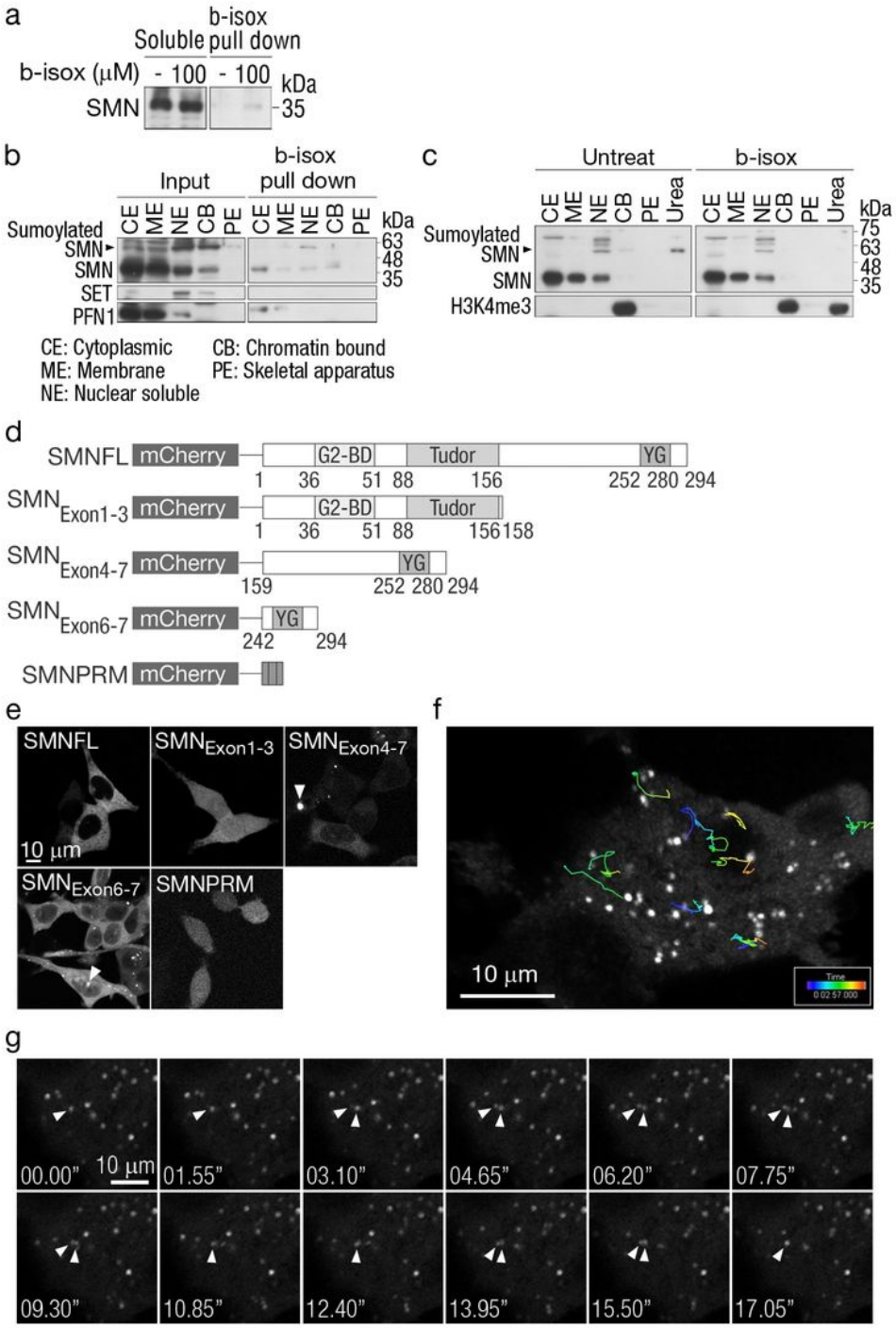

Figure 2

Identification of the prion-like domain of SMN a, b-isox precipitates SMN proteins from mes23.5 cells. b, Analysis of the cross-β conformation levels of SMN and PFN1 in different subcellular fractions of 293T cells. c, Results of fractionated proteins from cell lysates treated with or without b-isox are shown. d, Schematics of SMN mutants. e, Subcellular localization of SMN variants. Scale bar, 10 μm. f, Trajectory of granules derived from mCherry-SMNexon6-7. mCherry-SMNexon6-7 forms dispersed visible granules in

the cell. Scale bars: 10 μm. g, Images of the fission and fusion of mCherry-SMNexons6-7-derived granules. Visualization of supramolecular mCherry-SMNexons6-7 proteins by time-lapse microscopy and images of cells expressing mCherry-SMNexons6-7 taken every 1.55 sec for 17.05 sec. The arrowheads in the high-magnification images show the collision and separation of two distinct granules. Scale bars: 10 μm.

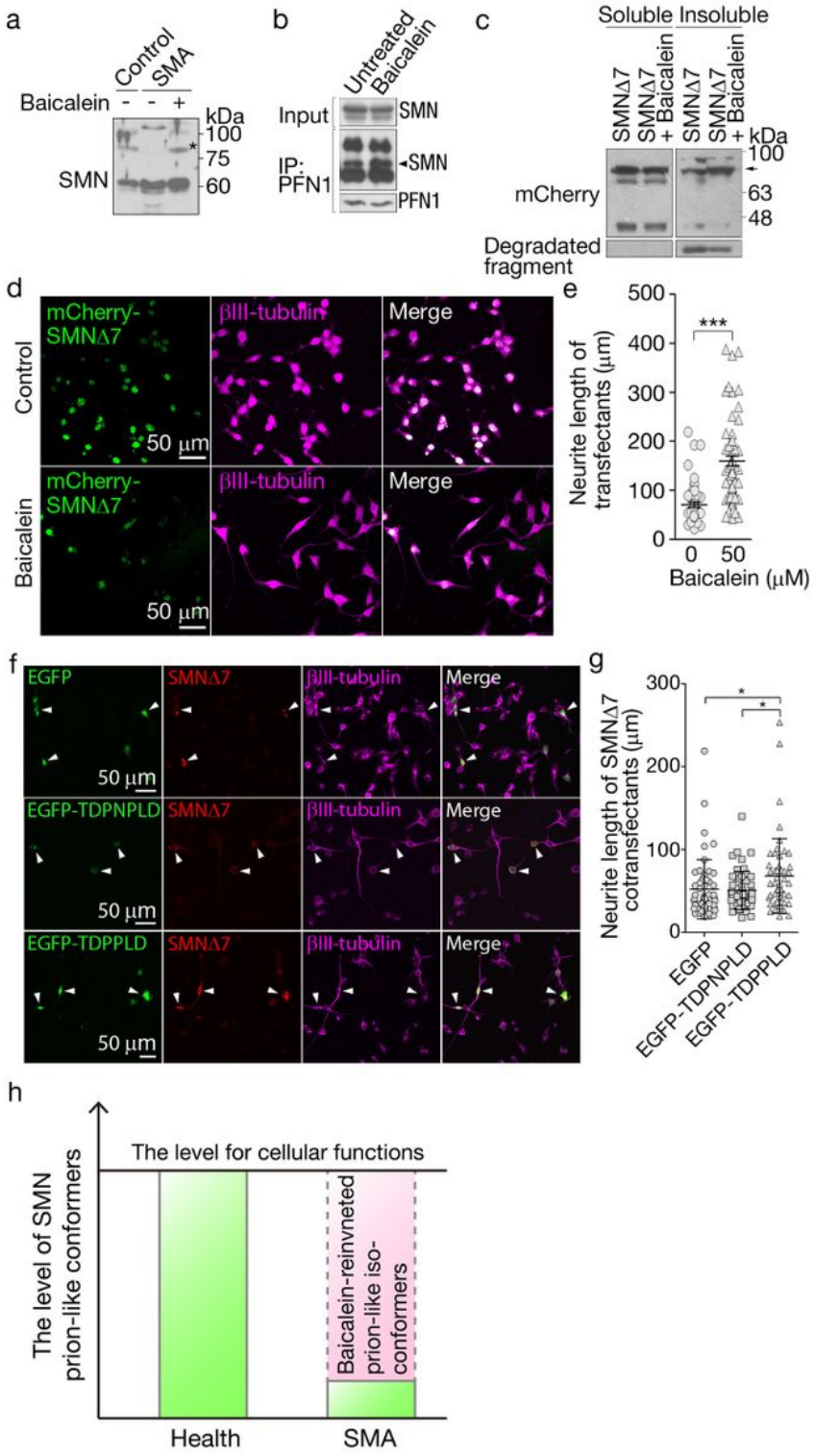

Figure 3

The pharmacological mechanism of baicalein in SMA. a, Western blotting reveals the in vivo cross-β assay of SMN in WT and SMA patient-derived HDFs treated with or without baicalein. * indicates the baicalein-corrected structure of SMN. b, The physical interaction of SMND7 with PFN1 was examined in the presence of baicalein. c, Baicalein attenuates the degradation of the SMND7 protein. d, Effects of baicalein on the axon length of cultured NSC34 motor neurons. Baicalein (50 mM)- or mock-treated NSC34 cells were stained with the bIII-tubulin antibody (purple). SMND7-transfected cells are shown by the red mCherry signal. Scale bar, 50 μm. e, Quantitation of the neurite length of SMND7-transfected cells. Statistical comparisons were performed using two-tailed Student's t-tests. All data are presented as the means with the SD (n = 3). *** $p<0.001$ f, NSC34 cells cotransfected with SMND7 and TDP-43 variants (indicated by arrows) were stained with the bIII-tubulin antibody (purple). Scale bar, 50 μm. g, Quantitation of the neurite lengths of cotransfected cells. Statistical comparisons were performed using two-tailed Student's t-tests. All data are presented as the means with the SD (n = 3). * $p<0.001$. h, Modeling of the prion-like conformation-based therapies for treating SMA with baicalein.

Supplementary Files

This is a list of supplementary files associated with this preprint. Click to download.

- FigS1.jpg
- FigS2.0.jpg
- FigS3.jpg
- FigS4.jpg
- WangSI.docx